Experimental and Numerical Analysis of Heating Performance of a New Skirting Board Radiator with Forced Air Circulation

Rahmati, Ahmad Reza*[+]; Gheibi, Ali; Karimpour, Rostam
Department of Mechanical Engineering, University of Kashan, Kashan, I.R. IRAN

ABSTRACT: *The thermal performance of a new modified hydronic skirting board heating system with an air supply is investigated in the present work. In the modified system indoor airflow is forced through a duct that is located between the systems. The main aim of the present work is to achieve a system with higher efficiency and lower energy consumption than conventional cases. The heat output rate of the system is evaluated experimentally for different water flow rates and inlet water temperatures based on standard No. En-442. A comparison of the results between the new system and the conventional models shows that heating performance improved by about 23%. Thermal comfort conditions in the room are analyzed according to Fanger's method and results show that people's dissatisfaction (PDD) in the different parts of the room is less than 40%. Also to validation of the numerical results, the temperature distribution of the simulation is compared with experimental data and obtained results show that there is a good agreement between them.*

KEYWORD: *Skirting board radiator, Air supply; Simulation, Thermal comfort conditions; Energy. consumption.*

INTRODUCTION

Statistics show that in 2020, the world population has grown by over 7.5 billion. Increasing population also means increasing energy consumption. Due to the reduction of non-renewable resources such as oil and gas, saving on these sources is especially important. The use of fossil fuels is increasing in the winter season (40% of total energy consumption) [1]. So designing high-efficiency and low-energy heating systems is one of the most effective ways to save energy. Panel radiators, skirting board heating systems, and underfloor heating are common heating systems that are used today. Most important of all is the performance. Underfloor heating offers slow warmth which isn't capable in colder temperatures, while the heating provided by skirting boards is similar to that of radiators. It takes a few minutes to heat up. Skirting board radiators have uniform heating distribution because of their location throughout the environment.

Based on the supply water temperature, there are three categories of the water temperature range for heat emitters, 1- High temperature (90 °C), 2- Medium temperature (60 °C), 3- Low temperature (45 °C).

Skirting board radiators with a medium system temperature have been proven not only to allow energy saving but also to create better thermal comfort conditions

***** *To whom correspondence should be addressed.*
+ E-mail: ar_rahmati@kashanu.ac.ir
1021-9986/2022/7/2428-2439 9/$/5.09

than high-temperature systems [2, 3]. Among the most important studies that are done in the field of skirting board radiators, Polaskic's work at KTH University in Sweden is more index [4-10]. *Polaskic* and *Holmberg* [6] investigated the specific geometry of the skirting board radiators, which are widely used in Sweden and the United Kingdom. Each section of their system is joined in the corners with patented push-fit connectors. Also an investigation of the skirting board heaters with an integrated air supply in done by *Polaskic* and *Holmberg* [11]. They simulated a room and obtain the temperature distribution and heat output rate of the system. Their results show that the heat out rate of the skirting board radiator with air supply gave about 2.1 more heat output than the conventional model in the best situation. In their model, the outside air at -6 ℃ is sucked into the interior space and enters the room space after passing through the air channel. Also in this model, the fluid transfer pipes are located inside the channel. One of the disadvantages of this method is that the radiator front cover surface is not too warm due to the inserted pipes in the duct and insufficient contact with the front surface so heat transfer radiation is low in this model. Given the long history of using panel radiators in buildings, some researchers have investigated the performance of such systems. *Polaskic et al*. [12] studied the heating performance of a ventilation panel radiator. Their results showed that a ventilation radiator with 10l/s air flow and at 45℃ inlet water temperature can support the heat needed for a room area of 34m^2. In that study also outlet air was sucked into the inner room space. Similar work was done by *Myhren* and *Holmberg* [13]. The result indicated that the heat output rate of their new system is 20% improved compared with conventional models. They also studied the double-panel ventilation radiators [14]. Based on their results, a related radiator without a convector plate has the best heating performance with a 20-40 mm gap between the panels. The most important aim of almost previous research is that they have focused on improving the performance of existing systems without changing the whole system engineering of it. Skirting board radiators, which are a kind of decorative radiator, given the less space they occupy are a good option for modern today buildings. Therefore, attention to improving their design and operation so that they are easy to install and maintain while maintaining high heat efficiency with the lowest energy consumption is an important issue that should be considered. In the experimental study by *Gheibi* and *Rahmati* [15], a new skirting board heating system was identified and their results showed that the thermal output rate increased by about 32% compared to conventional models. Based on the reviewed projects, a comprehensive study on the geometry of the skirting board heating system which is following the air supply mechanism has been not carried out yet. The main novelty of this work is related to the unique geometry of the modified radiator and also creating airflow between the radiator's fins. In the new geometry by changing the material of the pipes and using new geometry, the contact surface between the pipe and the cover is increased so both radiant and convection heat transfer are increased. Forced airflow into the system using the fan is done to help the air circulation in the room as much as possible and the system works with maximum efficiency at low temperatures.

NEW MODEL PRESENTATION

Different parts of the modified baseboard radiator can be seen in Fig. 1. Using copper pipes, due to the high heat transfer coefficient, causes high heat transfer from the water to the pipe surface. Aluminum clips establish the connection between the pipes and the cover surface. The width of the clips is 5 cm and to achieve the appropriate air circulation, the distance between them is also 5 cm. directing airflow to the interior space and preventing heat loss from the wall is done by up blades. The airflow is supplied by a centrifugal blower that is shown in Fig. 2. Netted air duct is installed between the pipes for direct airflow. To increase heat transfer and keep warm the inner compartment of the duct, is made of low-thickness aluminum. Exhaust air from the blower enters the preheated chamber before entering the air duct. An electrical heating silicon element is used in the preheated chamber. This type of element has high-temperature tolerance. There are several holes on the outer surface of the air duct. Exhaust air from the holes enter the environment after hitting the pipe surface.

EXPERIMENTAL SECTION

The heat output rate of the modified system is measured according to the European standard Norm En - 442. All experimental tests were performed in a standard test room with the following internal dimension.

1- Length (3m)
2- Width (3m)
3- Height (3m)

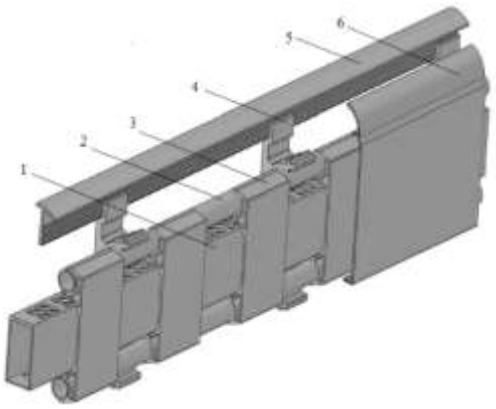

Part	Name	Material
1	Air duct	Aluminum
2	Pipe	Copper
3	Clips	Aluminum
4	Clamp	Plastic
5	Up blade	Aluminum
6	Cover	Aluminum

Fig. 1: Different components of the new modified skirting board.

According to En - 442, room temperature should be kept constant (20℃) so the test room walls are constructed with sandwich panels cooled by water. Different thermometers are installed at several points in the test room as Fig. 9. A diagram chart of the experiment process is shown in Fig. 3. The hot water required by the system is supplied by the hot water source which is heated by the electrical heater. Hot water enters the upper pipe of the radiator by a pump. A flow meter is installed at the water inlet path from the pump to the radiator and with a bypass flow, the inflow rate is adjusted. The length of the installed radiator in the room is 3 m. Figs. 4a-b show the test room and the installed systems in it. At first, to test, the water flow rate is fixed by a flow meter then outlet water temperature is measured at different inlet water flow rates. All measuring instruments are calibrated to reduce errors in testing. The temperature of the test room was also kept constant at 20° C. The required hot water is supplied by a tank with a heater 2000 W. During the test, the blower and the preheating chamber elements are permanently on.

As can be seen from Fig. 4a, two thermometers are installed at the inlet and outlet of the radiator. Heat transfer between the pipes and air duct and also the surrounding environment causes the temperature of the outlet water reduced. Of course, to install this system in real buildings the blower must be installed inside the wall, but in the test room, the blower was placed outside the wall because of the wall insulation. Fig. 4b, shows the installed radiator in the test room. The duct is made of aluminum with a thickness of 0.7 mm. There are several holes on the up and bottom surfaces of the duct. Also, the length of the duct before entering the skirting board radiator is assumed to be an extended flow regime.

FORMULATION

Total heat output from a hydronic radiator is dependent on three parameters: water flow rate, size of the radiator, and temperature difference between the radiator and ambient air. Heat output rate can be obtained by a global energy balance as Eq. (1), [16].

$$\dot{q} = \dot{m}_{water} c_{p-water} (T_{supply} - T_{return}) \approx U A_s \Delta T_{exc} \qquad (1)$$

The first part on the right-hand side of Eq. (1) is known as the steady-flow energy equation. It is the enthalpy change of the system. The second part of the right-hand side of Eq. (1) is known as Newton's Law of cooling. It is the ability to exchange heat energy between the system and its surrounding space. In Eq. (1), U is the total heat transfer coefficient of the radiator ($W/m^2.℃$), as is the heat exchange surface (m^2) and ΔT_{exc} is the logarithmic excess temperature. Eq. (2) shows the logarithmic excess temperature [17].

$$\Delta T_{exc} = \frac{T_{supply} - T_{return}}{\ln((T_{supply} - T_{room})/(T_{return} - T_{room}))} \qquad (2)$$

The total heat transfer coefficient can be presented as Eq. (3). α_{water} Is the convective heat transfer coefficient between water and the wall and α_{air} is the convective heat transfer coefficient between the wall and surrounding air. $\alpha_{water} >> \alpha_{air}$, so total heat transfer depends on the α_{air}.

$$U = (\alpha_{water}^{-1} + \alpha_{air}^{-1})^{-1} \qquad \alpha_{water>>}\alpha_{air} \qquad (3)$$

Reynolds number inside the duct can be obtained from Eq. (4). v_{air} is the mean air velocity inside the duct. D_h is the hydraulic diameter of the duct [17-18].

$$Re = \frac{\rho_{air} D_h v_{air}}{\mu_{air}} \qquad (4)$$

(a) (b)

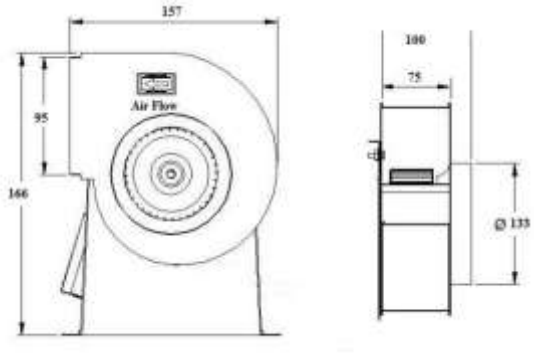

Capacitance (μF)	Air volume ($^{m^3}/_{h}$)	Speed ($^{r}/_{min}$)	Input (W)	Current (A)	Frequency(Hz)	Motor
2	252	2550	51	0.23	50	FTP 2E-92/5

Fig. 2: (a) Centrifugal blower connected to the skirting board heating system, (b) Technical scheme of the blower.

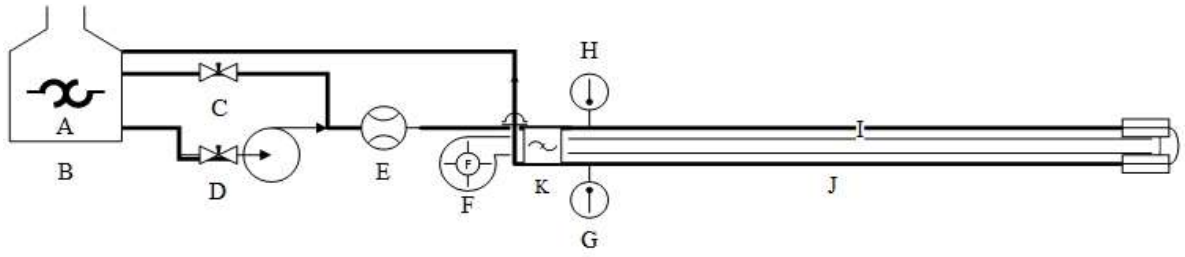

A: Heater, B: Water reservoir, C: Valve, D: Pump, E: Flowmeter, F: Centrifugal fan, H&G: Thermometer, I: Air duct, J: Skirting board radiator, K: Preheating chamber

Fig. 3: Diagram chart of the testing steps.

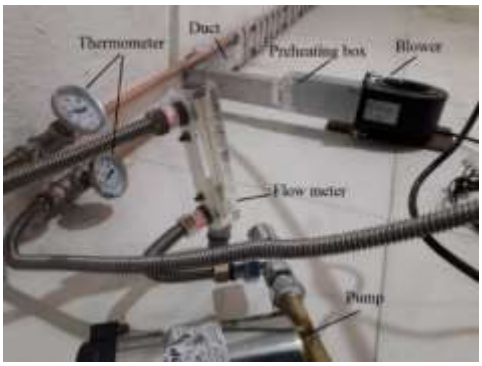

(a) (b)

Fig. 4: (a) Measuring instruments in the test room, (b) The installed air duct between the pipes.

$$\Delta D_h = \frac{4A_{duct}}{P_{duct}},\quad \mu_{air} = 1.458\times10^{-6}\ \frac{\sqrt{T_{ave}}}{1+\frac{110.4}{T_{ave}}} \qquad (5)$$

$$T_{ave} = \frac{T_{inlet,air} + T_{outlet,air}}{2}$$

In thermal convection cases, the Richardson number plays an important role in determining the Nusselt number. Richardson number can be estimated as Eq. (6) and is the importance of natural convection relative to forced convection. The Richardson number can also be expressed by using a combination of the Grashof number and Reynolds number as Eq. (7).

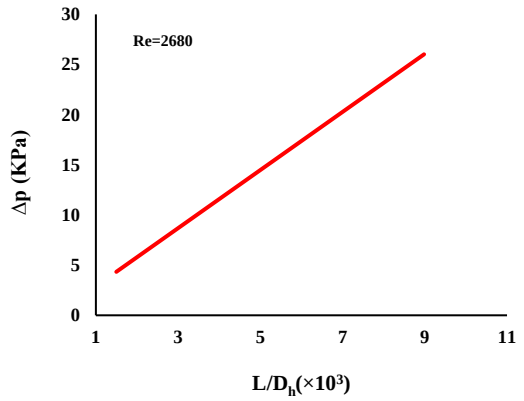

Fig. 5: Pressure loss of the air in the duct.

$$Ri = \frac{g\beta(T_s - T_{room})D_h}{\nu_{air}} \quad (6)$$

$$Ri = \frac{Gr}{Re^2} \quad (7)$$

In Eq. (6), β is the thermal expansion coefficient (equal to approximately $1/T_{ave}$). Typically, the natural convection is negligible when $Ri \ll 1$, forced convection is negligible when $Ri \gg 1$, and neither is negligible when $Ri \approx 1$. Nusselt number is determined based on Richard's number and Prandtl number. Prandtl number can be obtained as Eq. (8).

$$Pr = \frac{c_{p,air}\,\mu_{air}}{\kappa_{air}} \quad , \quad \kappa_{air} = 0.0241 + 0.0007T_{ave} \quad (8)$$

In Eq. (8), $c_{p,air}$ is the specific heat of the air, μ_{air} is dynamic viscosity and κ_{air} is the thermal conductivity of the air that is depended on the temperature and can be obtained from the presented equation in Eq. (8), [19]. Pressure loss of the air during the duct path is estimated as Eq. (9) and is shown in Fig. 5. It is assumed that air velocity is constant (10m/s) in the duct and the average air temperature is 27.5℃. Analytical calculation showed that the Prandtl number is 0.71. The range of the Reynolds and Richardson numbers are $1.1 \times 10^4 < Re < 2 \times 10^4$ and $4 \times 10^{-5} < Ri < 2 \times 10^{-4}$. This range is because of changing air velocity and the average temperature of the air along the duct.

$$\Delta p = f\frac{L}{D_h}\frac{\rho v^2}{2} \quad (9)$$

In Eq. (9), f is the friction coefficient of the duct that due to the turbulence regime of the flow can be predicted as Eq. (10), [20].

$$f = (1.82\log(Re) - 1.64)^{-2} \quad (10)$$

In turbulent flow, the experimental relationship for Nusselt number is developed as Eq. (11). It is assumed that the flow is thermodynamically and hydraulically developed. Nusselt number consists of three parts: 1-heat transfer rate, 2- entrance correction factor, 3- coefficient of fluid properties correction [11].

$$Nu = \frac{0.125f\,(Re - 1000)Pr}{1 + 12.7\sqrt{0.125f}\left(Pr^{2/3} - 1\right)} \times \left(1 + \left(\frac{D_h}{L}\right)^{2/3}\right)\left(\frac{T_{ave}}{T_s}\right)^{3/8} \quad (11)$$

The total convective heat transfer coefficient of the system can be approximated by Eq. (12).

$$\alpha_{air} = Nu\,\lambda_{air}\,D_h^{-1} \quad (12)$$

RESULTS AND DISCUSSION

The experiment was conducted in four parts for different water flow rates. In each part, heat output rates at seven different inlet water temperatures are obtained. Figs. 6a-d, show the results of the measurement of the radiator output temperatures relative to the inlet water temperature. Results show that the higher the inlet water temperature, the higher the difference between the inlet and outlet water temperatures. Measurement of the outlet water temperature is done three times. The average standard deviation is calculated based on Eq. (13) and is shown in Fig. 6.

$$\sigma = \left[\frac{1}{N-1}\sum_{i=1}^{N}(\theta_i - \bar{\theta}_i)^2\right]^{0.5} \quad (13)$$

In Eq. (13), $\bar{\theta}_i$ is the average temperature of the different measurements and σ is the standard deviation.

Figs. 7a-d show the radiator heat output rates relative to supply water temperature at different water flow rates. The preheating chamber temperature was kept constant at about 80 ° C. Air flow rate of about 10 l/s at the inlet is used to investigate the heating performance of the modified system. As can be seen from Fig. 8, the heat transfer rate increases as the water flow rate and supply water temperature increase. As the inlet water temperature increases, the heat exchange rate of the system with the environment will also increase. A comparison between the thermal

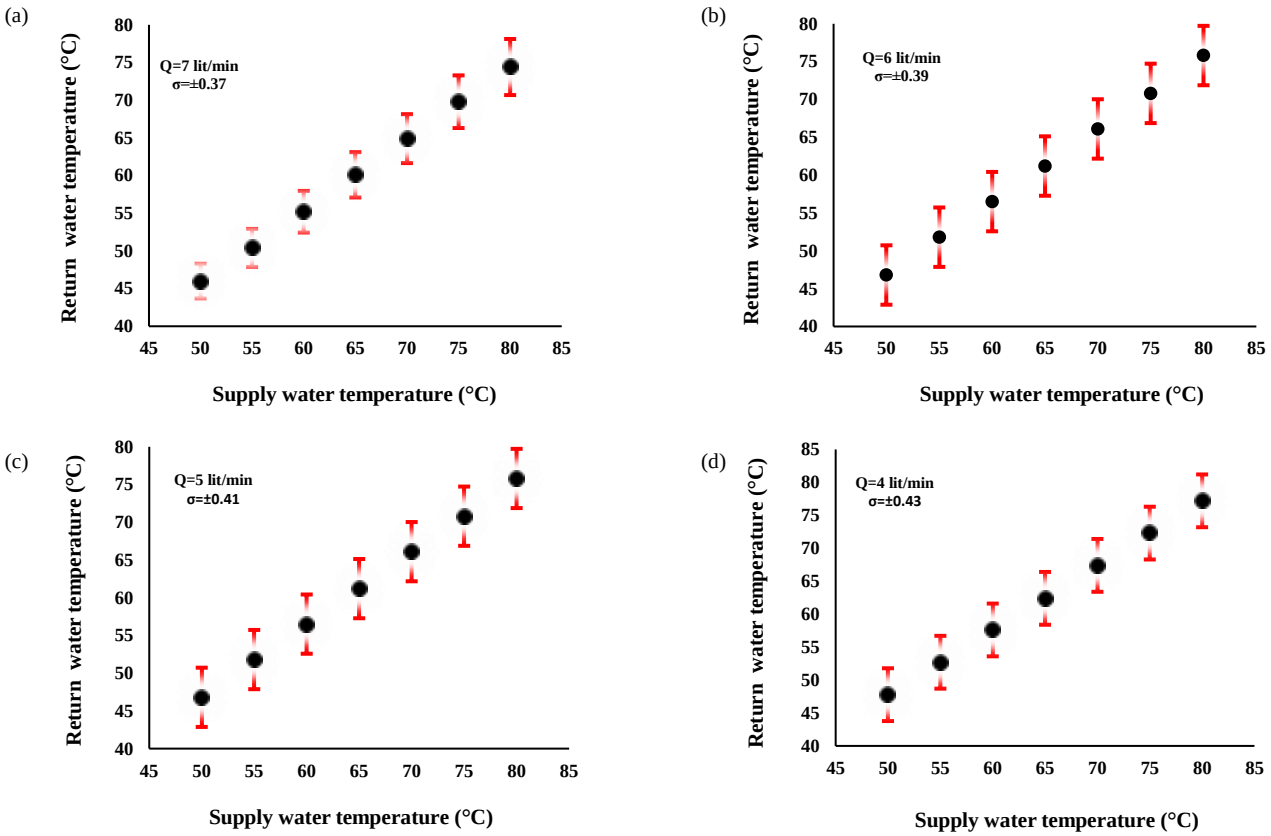

Fig. 6: Outlet water temperature relative to inlet water temperature at different flow rates. (a) Q=7 l/min, (b) Q=6 l/min, (c) Q=5 l/min, (d) Q=4 l/min.

the efficiency of the new modified system and conventional skirting board radiator with air supply (Ref. [11]) and other conventional models [6&15] is done and is shown in Fig. 8. Comparisons are done at 55℃ inlet water temperatures for two different water flow rates. As can be seen, the heat output rate from the new radiator enhanced by about 23% compared with the conventional model with an air supply and about 75% compared with the conventional models without an air supply. One of the most important advantages of the new radiator is the use of copper pipes for fluid transfer. The low specific capacity of the copper causes the heat transfer between the pipes and the air to occur rapidly. Also using aluminum clips causes more heat transfers from the pipes to the duct. The use of an indoor blower allows for better circulation of indoor air, which increases the speed of warming up.

Thermal comfort conditions

Thermal comfort conditions, which express a euphoric sense with the residents are an important aspect of the new building design because nowadays people spend most of their time in the building spaces. BS EN ISO 7730 describes thermal comfort conditions which express satisfaction with the thermal environment. Proper conditions are situations where people do not feel too cold or too hot. In this work, temperature distribution and thermal comfort conditions of the modified baseboard heating systems are calculated by simulating a room model in Flovent software. The main reason for using this software in this work is the ability to the simulation of the thermal comfort conditions based on Fanger's model. Temperature distribution in the room is obtained by solving the equations for heat and fluid flow. Indoor thermal radiation is simulated and emissivity factors for the internal walls and skirting board surface are 0.85 and 0.9, respectively.

The important conditions that are considered in the simulation method are as follows:

1- The initial temperature of the room is 8℃.

2- Results are presented for two hours after the system is turned on.

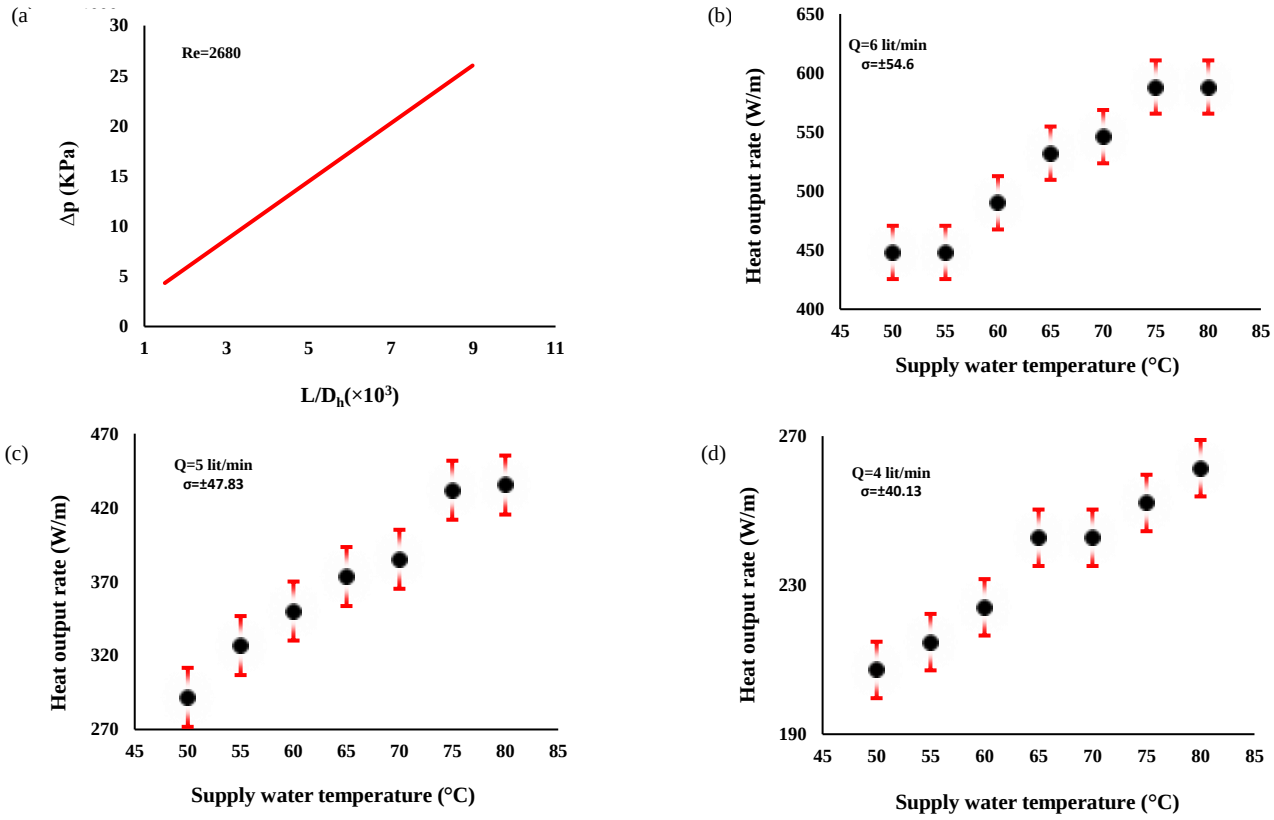

Fig. 7: Heat output rate of the radiator for different flow rates. (a) Q=7l/min, (b) Q=6l/min, (c) Q=5l/min, (d) Q=4l/min.

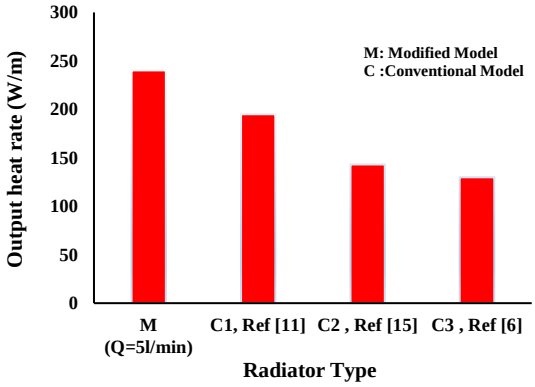

Fig. 8. Comparison of the output heat rates between the modified new model and conventional models with air supply and without it.

3- The air volume flow rate in the duct is 10 l/s.

4- The size of the duct cross-section and the height of the skirting board are given as their actual values (0.15m).

5- Several holes with a distance of 1cm above and below the duct are considered.

Fanger's Predicted Mean Vote (PMV) is used to analysis of the thermal comfort conditions [21]. In this model, the seven-point ASHRAE thermal sensation scale (-3 to +3 from cold to hot) can make a difference between thermal sense. The PMV model depends on six parameters consisting of air temperature and velocity, mean radiant temperature, relative humidity, clothing insulation, and activity level. Table 1 shows the recommended standard thermal comfort conditions in the cold season presented by ASHARE standard No.55 [22]. Fanger's equation as shown in Eq. (13) is the relation between PMV and thermal load. In Eq. (13), ξ is the rate of metabolic production per surface area and ϱ is the thermal load on the human body. In the present study, the metabolic rate is 93 W/m^2.

$$PMV = 3.155\varrho(0.303\xi + 0.028) \quad (13)$$

In Fanger's model, people dissatisfaction (PDD) is the presence of people who are not comfortable with ambient temperature conditions. Eq. (14) shows the empirical equation between the PMV and PDD.

$$PDD=100-95\exp\left(-0.03353PMV^4 - 0.2179PMV^2\right) \quad (14)$$

Fig. 9 Shows the validation of the software temperature distribution in the room with experimental. As can be seen

Table 1: Thermal comfort conditions based on the ASHARE standard 55(1992) [22].

Optimum temperature	Acceptable temperature range	Assumptions for other PMV inputs
22℃	20-23℃	Relative humidity: 50% Mean relative velocity: <0.15m/s Mean radiant temperature:=Air temperature Metabolic rate: 12 met Clothing insulation: 0.9 clo

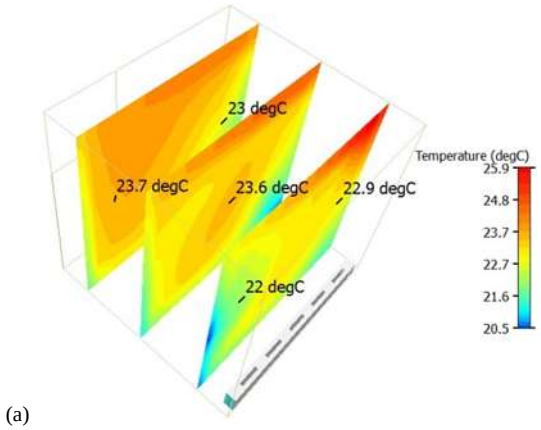

(a)

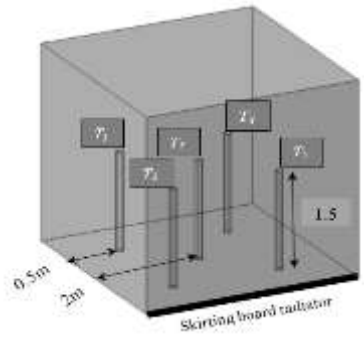

(b)

Experimental	T_1	T_2	T_3	T_4	T_5
	22	21	23	21.5	21.9
Error (%)	7	4	2	6	4

Fig. 9: Validation of the temperature distribution results (a) simulation in Flovent software, (b) Locating the thermometers installed in the test room.

from Fig. 9b, five thermometers are installed in the room and the obtained temperatures from them are compared with the simulation results. In the simulation and experimental inlet water temperature is 60℃ and the airflow rate is 10 l/s. The initial room temperature is 10 ℃ and the system is powered on for 2 hours. Fig. 10a shows the related temperature of the simulation result corresponding to the location of the thermometers in the test room. As can be seen, the average difference between the results is less than 5%.

Also, there was experimental work on floor heating systems by *Omori* [23]. In that work the floor area is 25m^2 and other important parameters for the building and heating system are as Table 1 in Ref. [23]. The following figures show the temperature distribution of the room at two different positions. As can be seen, there is good agreement between them. By performing a simulation-like process for underfloor heating systems, the new modified system is simulated. Supply water temperature is 50℃ and ambient temperature is adopted from TRNSYS software weather data following the test date in the laboratory. The initial room temperature is 10℃ and it is assumed that the system is working for 2 hours. Fig. 10, shows a comparison between the simulation and experimental results.

The simulated room has dimensions 3m×3m×3m. Wall thickness is 0.1 m and their conductivity is 1.63 W/m.K. Wall functions have been used to increase the accuracy of calculations in the intended mesh. Local mesh refinement is applied near the walls where there are more intense gradients. Transfer from refined mesh near the walls toward the center of the room is done smoothly. Fig. 11 Shows the simulated room and the computational domain which is considered in the simulation. The surface radiator material is aluminum anodized with specific heat 913 J/kg.K. To numerical investigation, there will be a certain number of elements beyond which the accuracy cannot be improved, and until the deviance becomes constant, a grid independence study was carried out. In this study, the temperature of the central point of the room is considered the main criterion for determining the number of cells. Fig. 12, shows the grid study results. As can be seen from Fig. 12, using 2950 cells grid independence will be achieved.

Figs. 13 and 14 show temperature distribution and people's dissatisfied percent in different sections of the room. Due to high density, cold air is located near the floor of the room. Placing the radiator heating system nearby

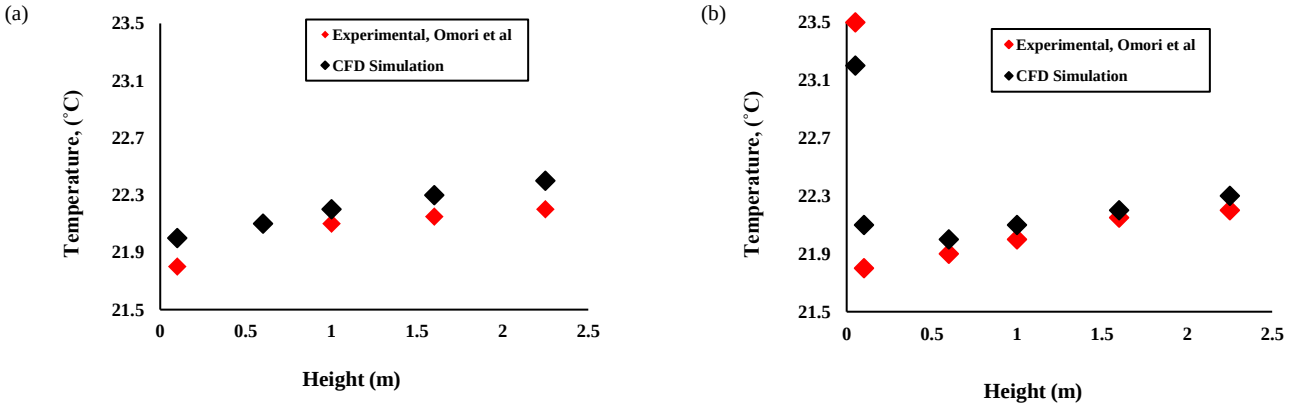

Fig. 10: Comparision between the experimental (Ref.[23]) and simulation of the temperature distribution across the room height-floor heating system , (a) x(room width):2m and z(room length):0.4m, (b) x(room width):2m and z(room length):3.15m.

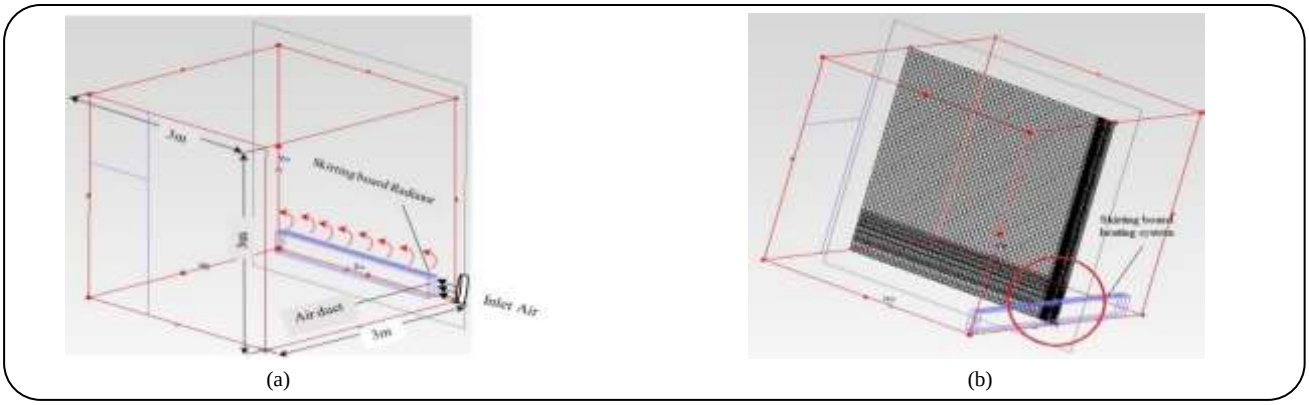

Fig. 11: (a) The simulated scheme consists of a room with a skirting board radiator and a fan, (b) a view of the meshing in the central section of the room.

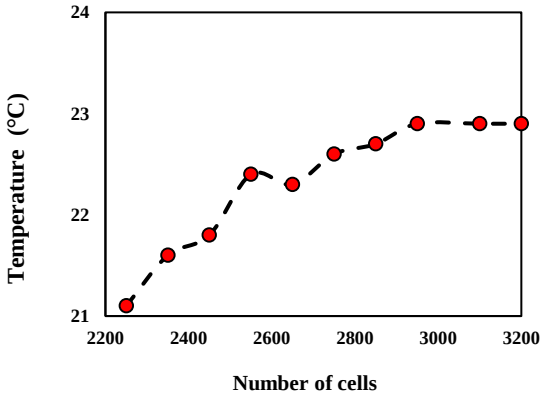

Fig. 12: Grid independence study.

will improve air circulation. The average temperature difference between different heights of the room is about 1°C. This system compared with the conventional model without an air supply can create a comfortable temperature in a room with less space. Also, as shown in Fig. 13, a strong temperature gradient is observed near the air outlet section, so by installing this system under the windows, it is easy to deal with cold airflow. As the results were shown in Fig. 14, the average PDD in the room with the new model is about 26%.

Fig. 15, shows the effect of thermal radiation and convection (natural + force) on the total heat emission. This study was conducted in different supply water temperatures and also different water flow rates at an air flow rate 10 l/s. In all cases, the convection heat transfer rate is significantly higher than the radiation heat transfer rate. As the supply water temperature and its flow rate increased, the radiation heat transfer rate increased too. The convection mechanism has a great influence on the water flow rate. Increasing the water flow rate will increase the convection heat transfer rate.

CONCLUSIONS

In this work, a new modified skirting board heating system with an air supply is analyzed experimentally.

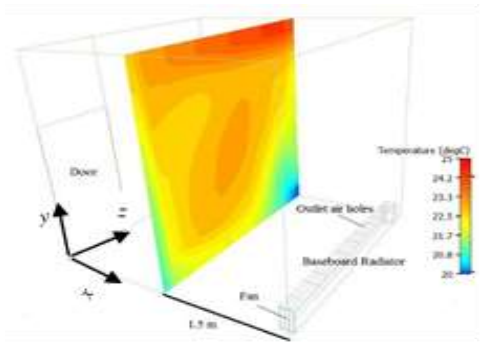

(a)

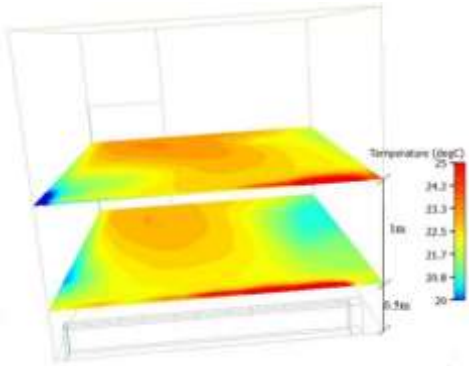

(b)

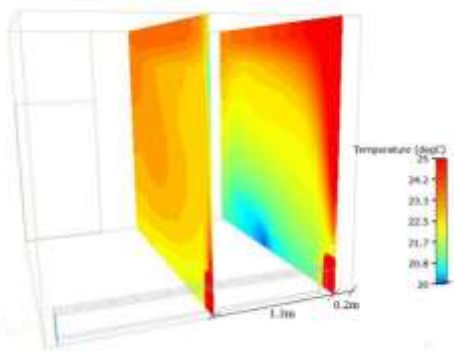

(c)

Fig. 13: Temperature distribution at different room sections, supply water temperature (45℃)-air flow rate (10 l/s), (a): x=1.5m, (b): y=o.5 & y=1.5, (c): z=0.2 & 1.5.

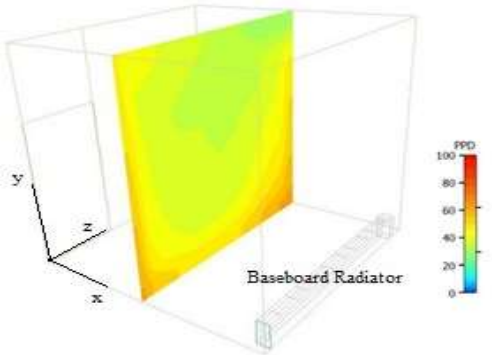

(a)

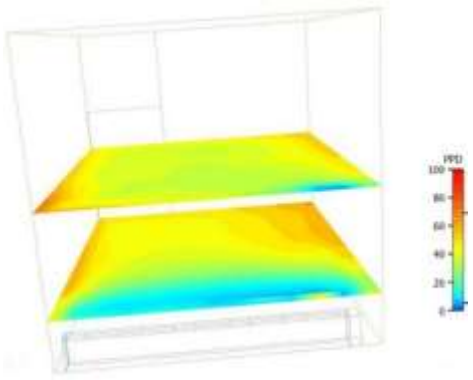

(b)

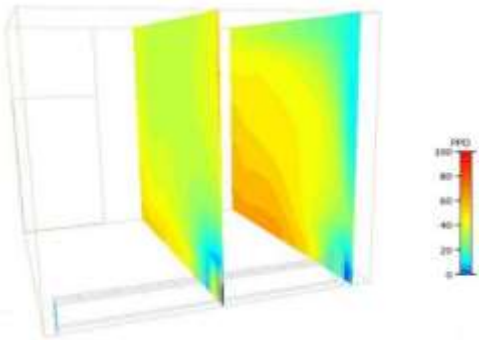

(c)

Fig. 14: PDD distribution in the room at different room sections, supply water temperature (45℃)-air flow rate (10 l/s), (a): x=1.5m, (b): y=o.5 & y=1.5, (c): z=0.2 & 1.5

Changing the material and geometric shape of the system is one of the innovations of the new system. Results show that as the supply water temperature and inlet water flow rate increased the output heat rate of the new modified system was enhanced. The heating performance of the new system in an airflow rate of 10 l/s and different supply water temperatures improves on average 23% compared to the conventional model. In the flow rate of 5 l/min and 55℃ of the inlet water temperature, modified system performance improved by about 67% compared with the conventional model without air supply at similar conditions in Ref. [11], also, 84% compared with the presented system in Ref. [6]. The convection heat transfer rate of the new system significantly is higher than the radiation

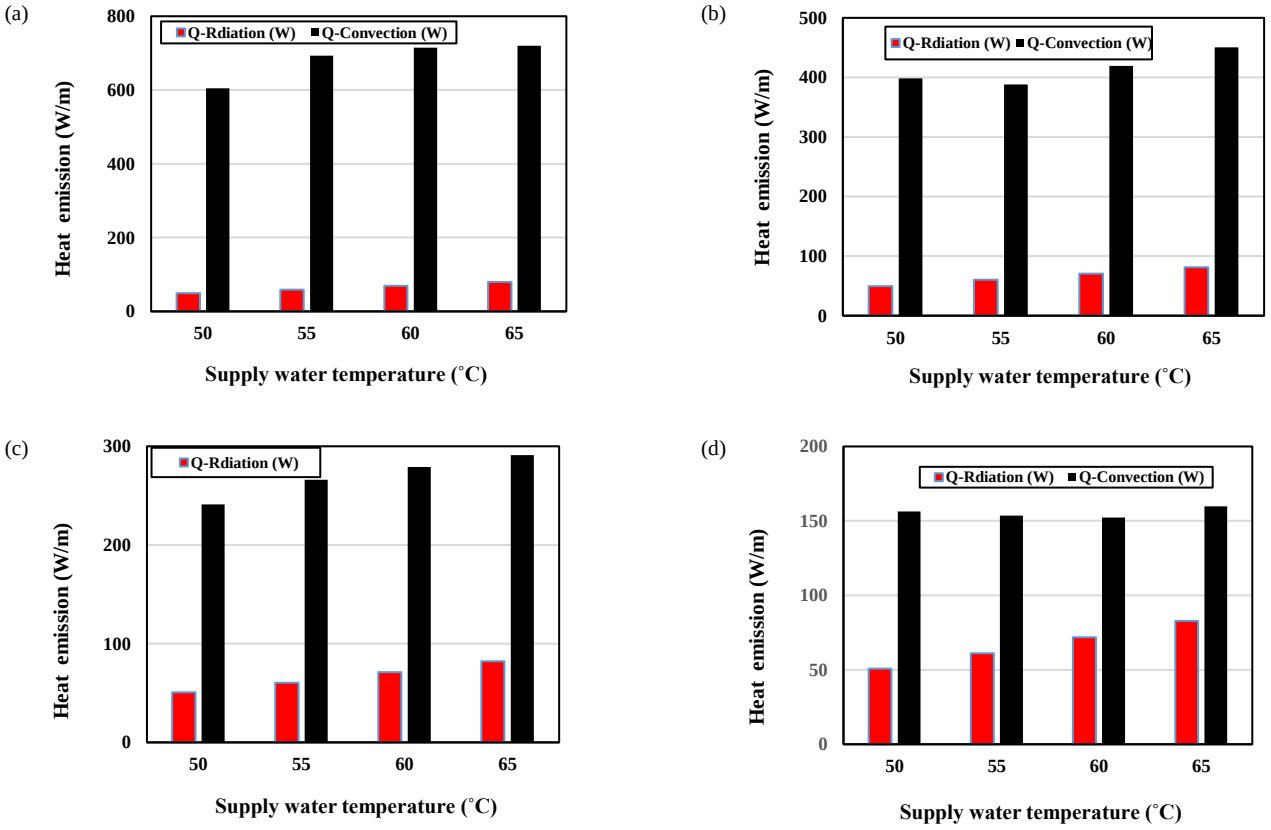

Fig. 15: Distribution of heat emission in the different supply water temperatures and flow rates, (a): 7 l/min, (b): 6 l/min, (c): 5 l/min, (d): 4 l/min.

heat transfer rate. Since thermal comfort in the environment depends on various parameters, the simulation of this system was done in software, and the temperature distribution of the system is obtained which is consistent with the results of the temperature distribution obtained from the experiment. Based on the temperature distribution of the systems and also other influential parameters, thermal comfort condition is analyzed and numerical results show that the new model was able to counter cold downdraught with a uniform temperature distribution in the room

Nomenclature

A_s	The outer surface of the skirting board, m^2
A_{duct}	The cross-section area of the duct, m^2
$C_{p\text{-}water}$	Specific heat capacity of water, J/kg.°C
D_h	Duct hydraulic diameter, m
f	Friction factor
g	Gravitational acceleration, m/s^2
Gr	Grashof number
L	Radiator length, m
$\dot{m}_{water}$	Water mass flow rate, kg/s
Nu	Nusselt number
P	Cross-section Perimeter of the duct
Pr	Prandtl number
$\dot{q}$	Output heat rate, W
Q	Water flow rate, L/min
Re	Reynolds number
Ri	Richardson number
T	Temperature, °C
v_{air}	Mean air velocity in the duct, m/s
U	Total heat transfer coefficient of the radiator $W/m^2.°C$

Greek letters

α	Convection heat transfer coefficient, $W/m^2.°C$
β	Air thermal expansion, 1/°C
μ_{air}	Air dynamic viscosity, kg/m. s
κ_{air}	Air heat conduction coefficient, W/m.°C
ϱ	Thermal load on the human body, W
ξ	Metabolic production rate, W/m^2

λ_{air} Air thermal conductivity, W/m. °C
T Temperature, °C
v_{air} Mean air velocity in the duct, m/s
U Total heat transfer coefficient of the radiator W/m^2. °C

Received : May. 25, 2021 ; Accepted : Aug. 30, 2021

REFERENCES

[1] Allard F., Buildings Energy Conservation: European Countries' Experience, F-17042, France.

[2] Eijdems H.H., Boerstra A.C., Op't Veld P.J.M, "Low-Temperature Heating Systems: Impact on Iaq, Thermal Comfort and Energy Consumption", In *Proceedings, Healthy Building 1994*, Vol. 94, (1999).

[3] Inard C., Meslem A., Depecker P., Energy Consumption and Thermal Comfort in Dwelling-Cells: A Zonal-Model Approach, *Building and Environment*, **33(5)**: 279-291 (1998).

[4] Ploskić A., Holmberg S., Heat Emission from Thermal Skirting Boards, *Building and Environment*; **45(5)**: 1123-1133 (2010).

[5] Ploskic A., "Technical Solutions for Low-Temperature Heat Emission In Buildings" Doctoral Dissertation, KTH Royal Institute of Technology (2013).

[6] Ploskić A., Holmberg S., Performance Evaluation of Radiant Baseboards (Skirtings) for Room Heating–An Analytical and Experimental Approach, *Applied Thermal Engineering*, **62(2)**:382-389 (2014).

[7] Ploskić A., Holmberg S., "Heat Emission from Skirting Boards–an Analytical Investigation", In *Proceedings of the 3rd International Conference on Built Environment and Public Health*, EERB-BEPH 2009At: Guilin - China 2009, (2009).

[8] Hesaraki A., Bourdakis E., Ploskić A., Holmberg S., Experimental Study of Energy Performance in Low-Temperature Hydronic Heating Systems, *Energy and Buildings*, **109**:108-14, (2015).

[9] Wang Q., Ploskić A., Holmberg S., Low-Temperature Heating in Existing Swedish Multi-Family Houses—An Assessment of the Significance of Radiator Design and Geometry, *Science and Technology for the Built Environment*, **23(3)**: 500-511 (2017).

[10] Wang Q., Ploskic A., Ganter N., Holmberg S., Indoor Environment and Energy Performance Evaluation of Low Temperature Heating in Retrofitting Existing Swedish Residential Buildings, *Building Simulation*, (2019).

[11] Ploskić A., Holmberg S., Low-Temperature Baseboard Heaters with Integrated Air Supply–An Analytical and Numerical Investigation, *Building and Environment*, **46(1)**:176-186 (2011).

[12] Ploskić A., Wang Q., Sadrizadeh S., A Holistic Performance Evaluation of Ventilation Radiators–An Assessment According to EN 442-2 Using Numerical Simulations, *Journal of Building Engineering*, **25**: 100818 (2019).

[13] Myhren J.A., Holmberg S., Performance Evaluation of Ventilation Radiators, *Applied Thermal Engineering*, **51(1-2)**: 315-324 (2013).

[14] Myhren J.A., Holmberg S., Design Considerations with Ventilation-Radiators: Comparisons to Traditional Two-Panel Radiators, *Energy and Buildings*, **41(1)**: 92-100 (2009).

[15] Gheibi A., Rahmati A.R., An Experimental and Numerical Investigation on Thermal Performance of a New Modified Baseboard Radiator, *Applied Thermal Engineering*, **163**:114324 (2019).

[16] Incropera F.P., Lavine A.S., Bergman T.L., DeWitt D.P., "Fundamentals of Heat and Mass Transfer", John Wiley & Sons, Inc. (2018).

[17] James A.F., "Introduction to Fluid Mechanics", Cambridge: MIT Press, MA; (1994).

[18] Crowe C.T., Elger D.F., Roberson J.A., Williams B.C., "Engineering Fluid Mechanics", 9th ed., John Wiley & Sons, Inc. (2008).

[19] Alvarez H., "Energiteknik (Energy Technology)", pp. 360-374, Chapter 5.3, (2003) [in Swedish].

[20] Gnielinski V., New Equations for Heat and Mass Transfer in Turbulent Pipe and Channel Flow, *Int. Chem. Eng.*, **16(2)**: 359-368 (1976).

[21] Fanger P.O., "Thermal Comfort. Analysis and Applications in Environmental Engineering", Copenhagen: Danish Technical Press, p. 244, (1970).

[22] Nicol J.F., Humphreys M.A., New Standards for Comfort and Energy Use in Buildings, *Building Research & Information*, **37(1)**: 68-73 (2009).

[23] Omori T., Tanabe S.I., Akimoto T., "Evaluation of Thermal Comfort and Energy Consumption in a Room with Different Heating Systems", *In IAQVEC 2007 Proceedings - 6th International Conference on Indoor Air Quality, Ventilation and Energy Conservation in Buildings: Sustainable Built Environment* (2007).